Struct Multidisc Optim (2009) 38:405–414
DOI 10.1007/s00158-008-0281-0

MEDICAL AND BIOENGINEERING APPLICATION

Three dimensional shape optimization of total knee replacements for reduced wear

Ryan Willing · Il Yong Kim

Received: 20 September 2007 / Revised: 25 April 2008 / Accepted: 28 April 2008 / Published online: 30 July 2008

Abstract This paper presents the design optimization of a total knee replacement (TKR) using a parametric three-dimensional finite element (FE) model, considering wear of the ultra high molecular weight polyethylene (UHMWPE) insert. A framework has been developed to generate three-dimensional FE models of the femoral component and UHMWPE insert of a TKR design in a batch mode process, then simulate an ISO standard TKR wear test. A modified version of Archard's wear model calculates abrasive wear as a function of contact pressure, sliding distance and an experimentally determined wear factor. The UHMWPE wear was reduced by modifying the contact geometry of both components in the frontal and sagittal planes. Wear was reduced by 18.5%, from 55.248 to 45.013 mm^3 per year by reducing the radii of curvature of the femoral condyles in the sagittal planes, increasing the radii in the frontal plane, and reducing conformity between the implant components.

Keywords Total knee replacement · UHMWPE wear · Finite element analysis · Design optimization · Contact analysis

1 Introduction

Total Joint Replacement is now a commonly used treatment for various bone degenerating diseases, estimated to be performed over 1.5 million times per year worldwide (Bills et al. 2005); however, the frequency of Total Knee Replacement (TKR) procedures in the United States alone is expected to reach almost 3.5 million per year by 2030 (Kurtz et al. 2006). Revision procedures are necessary if the artificial joint components become sufficiently damaged, loosened, or if they are rejected by the host.

Damage to the ultra high molecular weight polyethylene (UHMWPE) insert accounts for one of the leading causes of TKR revision (Sharkey et al. 2002). Cornwall et al. (1995) identified 7 mechanisms of polyethylene degradation in TKRs, including abrasion, delamination, pitting, scratching, burnishing, deformation and embedded debris. Abrasive wear is highly dependent on the design of the implant (McEwen et al. 2005), and not only causes damage to the implant itself, but also releases wear particles into the surrounding tissues. These wear particles have been shown to cause osteolysis (the active resorption or dissolution of bone tissue) at the bone-implant interface which leads to implant loosening (Revell et al. 1978). Abrasive wear is a function of contact pressure, material properties, and kinematics (Fregly et al. 2005), which indicates that the younger, more active patients receiving TKRs will be more prone to polyethylene wear related issues.

Computational models have been used extensively in artificial knee design. Explicit finite element models and elastic layer models are often used to predict contact pressures and joint kinematics during a gait cycle with reasonable results (Fregly et al. 2003; Godest et al. 2002; Halloran et al. 2005; Sathasivam and Walker 1998), while implicit finite element methods have been used to determine implant and bone stresses during static joint poses (Dargahi et al. 2003; Essner et al. 2003;

R. Willing · I. Y. Kim (✉)
Department of Mechanical and Materials Engineering,
Queen's University, Kingston, Canada
e-mail: iykim@me.queensu.ca

R. Willing
e-mail: willing@me.queensu.ca

Giddings et al. 2001; Sathasivam and Walker 1994; Au et al. 2005). Computational wear models have been used to predict damage caused by wear and creep (Fregly et al. 2005; Knight et al. 2007; Zhao et al. 2008), and subsurface damage (Sathasivam and Walker 1998), which compare well to observed polyethylene damage. Numerical modeling of wear testing machines reduces the costs associated with *in-vitro* testing and the destruction of prototypes.

Little design optimization has been attempted for TKR design despite its great potential in this field. Optimization of the bearing surfaces of a TKR in two-dimensions has been performed, considering the frontal and sagittal planes (Dargahi et al. 2003; Sathasivam and Walker 1994). A limitation of these studies is that wear estimates were only based on contact pressure, while recent work has shown that the contact pressure can be increased with reduced wear rates (Essner et al. 2003). As well, the two-dimensional simplifications of these models required that no axial rotation or torque could be applied.

In this study, the shape optimization of the articular surfaces of the femorotibial joint of a right-leg TKR is conducted using a three-dimensional finite element model, a wear model which takes sliding distance, contact area and contact pressure into account, as well as three-dimensional transient loading based on wear testing standards. This requires a framework for executing various engineering software packages in a batch process and facilitating information exchange seamlessly between them. This study produces a TKR design optimized for reduced wear while overcoming limitations of previous work.

2 Method

2.1 Total knee replacement

Total joint replacement is the replacement of the natural joint components with biocompatible metal alloys and polymers. For TKR, there are normally 4 components implanted at the knee (Fig. 1): femoral component, tibial tray, UHMWPE insert, and patella. The femoral component, normally cast from a cobalt-chromium alloy, replaces the distal femur. Anatomically shaped, the femoral component of a total knee has two highly polished condylar surfaces for the femorotibial joint which span from the distal to posterior surface, and a groove along the anterior surface for the femoropatellar joint.

The proximal tibia is normally replaced by a tibial tray (commonly titanium) which serves as a foundation

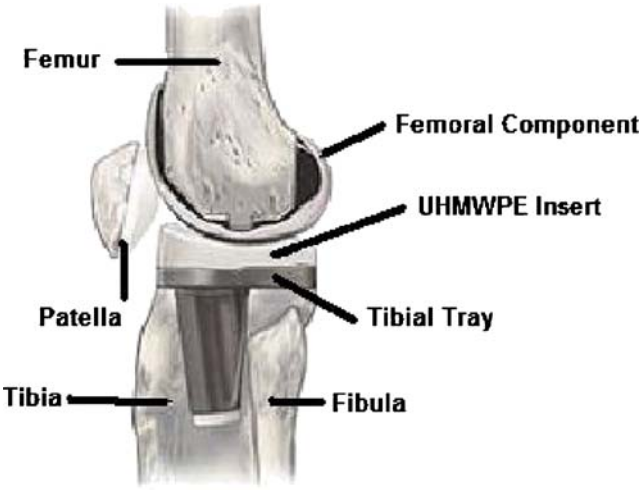

Fig. 1 Typical components of a TKR—adapted from Zhao et al. (2008)

for the UHMWPE insert. This insert acts as a cushion to distribute the load transfer from the femur to the tibia, as well as a low-friction surface to allow the necessary translations at the joint. The surface normally has two dished-out patches, to match the condylar profile of the femoral component, together forming the femorotibial joint.

The patella serves two purposes – to protect the front of the knee and to provide an increased moment arm for quadriceps forces. The natural knee cap is normally resurfaced with an UHMWPE replacement, designed to be compatible with the femoral component and complete the femoropatellar joint.

As noted in Section 1, there are several major failure modes for TKR; abrasive wear is one of the most important performance measures and can be assessed by wear testing of the femorotibial joint. The femoral component, tibial tray and UHMWPE insert are installed onto a testing machine capable of generating translations and rotations similar to those seen at a natural knee. An example is the ISO standard for knee wear testing, which simulates the loads and displacements seen during normal gait. A gait cycle can be broken down into a stance phase and a swing phase. During the stance phase, high joint loads are present with relatively low displacements. During the swing phase (when the foot would be off the ground), joint loads are relatively minimal, but much higher translations are present. Note that the patella does not play an important role in abrasive wear of the artificial joint.

2.2 Parametric finite element model

The finite element analysis (FEA) method is used in this study in order to perform numerical simulations, as

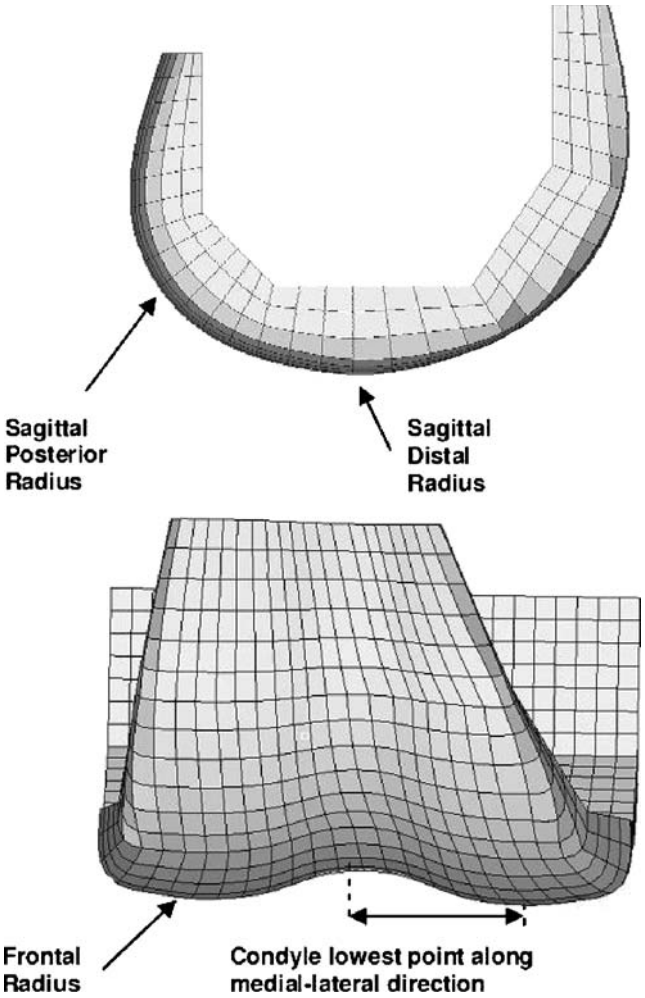

Fig. 2 Design variables of the TKR femoral component considered in this study (unused parameters not shown). All 4 variables shown can be modified separately for the medial and lateral condyles, resulting in 8 femoral component parameters

the derivation of an analytical method to analyze the contact geometry of a TKR is far too complex. Contact analysis is performed using the Augmented Lagrange method. In this study, the femoral component and polyethylene insert of a TKR are modeled using a bottom-up approach in the commercial FEA pre-processor Altair HyperMesh v 7 (Altair Engineering Inc., Troy, MI) for quasi-static simulations in the commercial FEA solver ANSYS v 9.0 (ANSYS Inc., Canonsburg, PA). Since the end goal of this model is a shape optimization, many of the dimensions are parameterized so they can be adjusted in order to simulate different designs.

Constructing a parametric finite element (FE) model presents quite a formidable challenge, as mesh quality and accuracy need to be maintained while changes in geometry occur. This is ensured through careful programming and consideration of many geometrical relationships, the use of powerful mesh controls within HyperMesh, and tedious debugging. While modeling the femoral component (Fig. 2) and the UHMWPE insert (Fig. 3), most facets of the geometry are parameterized and special care is taken to ensure mesh quality is maintained while different dimensions are modified.

The UHMWPE insert and cobalt-chromium femoral component are meshed with 8-node three-dimensional isoparametric linear brick type elements. The contact surface of the UHMWPE insert is meshed with ANSYS CONTA173 elements, and the contact surface of the femoral component is meshed with ANSYS TARGE170 elements, which together form an Augmented Lagrange surface-to-surface contact pair. The interface between the femoral component and the femur, as well as the interface between the UHMWPE insert and the tibial tray, are assumed to be rigid, and guided by the ANSYS Multi-Point Constraint (MPC) method. This allows both components to be guided by pilot nodes, where appropriate loads and degrees of freedom can be applied (Fig. 4). Information on these element types and the MPC method can be found in the ANSYS Theory Reference (ANSYS 2004).

A coefficient of friction of 0.04 between the two surfaces is assumed, as previous studies have reported good agreement with experimental data when using this value (Godest et al. 2002; Halloran et al. 2005). Non-linear elastic compressive properties of polyethylene in-vivo are derived from modulus-stress data by Cripton (1993). Assuming a bi-linear fit to that data and solving the first order differential system allows for the derivation of the stress-strain relationship used in the present study (Fig. 5). A Poisson's ratio of 0.44 for UHMWPE is used. The stiffness of the CoCr femoral component is assumed to be 230 GPa with a Poisson's ratio of 0.32.

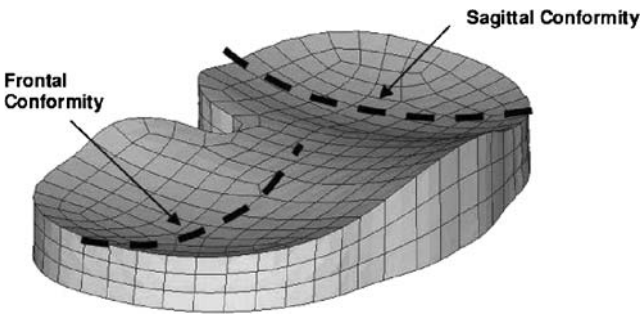

Fig. 3 Design variables of the TKR UHMWPE insert considered in this study (unused parameters not shown). Frontal and sagittal conformity assumed the same for medial and lateral condyles (although radius of dish area on insert in either plane will vary depending on the corresponding femoral condyle's distal and frontal radii)

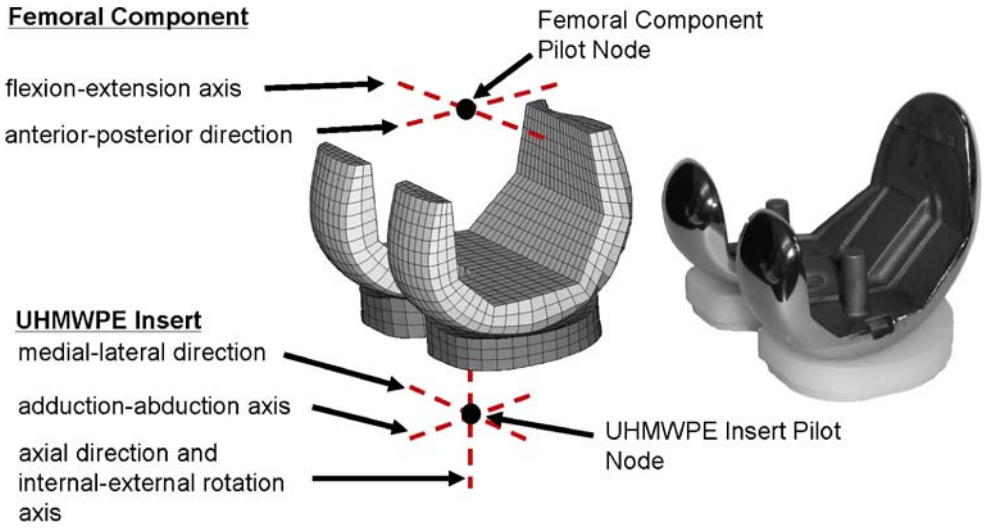

Fig. 4 Pilot node positions and degrees of freedom defined. These pilot nodes were positioned in order to match centres of rotation of a wear simulator about the different axis, including the 5 mm medial offset of the adduction-abduction axis of the UHMWPE insert pilot node

A mesh convergence study determined that a mesh of 5000 elements was sufficient when considering wear. Further increase in mesh density resulted in no change to the predicted wear volume or distribution. No wear iteration convergence study was performed, as only one wear iteration was considered. Considering that the model is intended for an optimization study, and single iteration function evaluation times approach 1 hour, this was a necessary simplification. Certain aspects of the model are validated by simplifying the contact geometry to a sphere-on-flat situation and comparing the FE model results to analytical Hertz stress results (Johnson 1985).

2.3 Loads and boundary conditions

The loading during simulation is based on ISO 14243-1 (1999) (Fig. 6), a TKR wear test for use with force controlled joint simulators. These machines typically feature springs to represent soft tissue constraint which is normally present at the knee. In order to include these effects, a translational spring with a stiffness of 30 N/mm against anterior-posterior relative motion of the components, and a torsional spring with a stiffness of 0.6 Nm/deg against internal-external relative rotation of the components are included. Flexion-extension

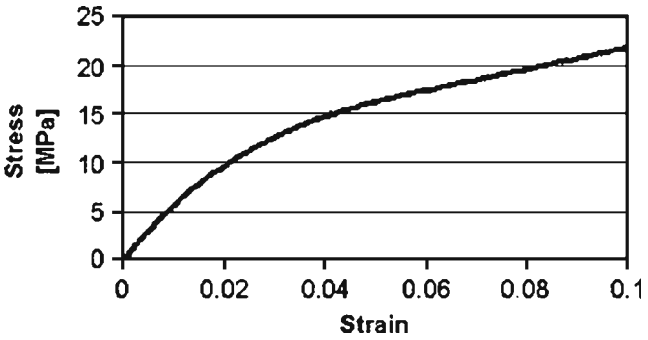

Fig. 5 Compressive stress-strain relationship of UHMWPE

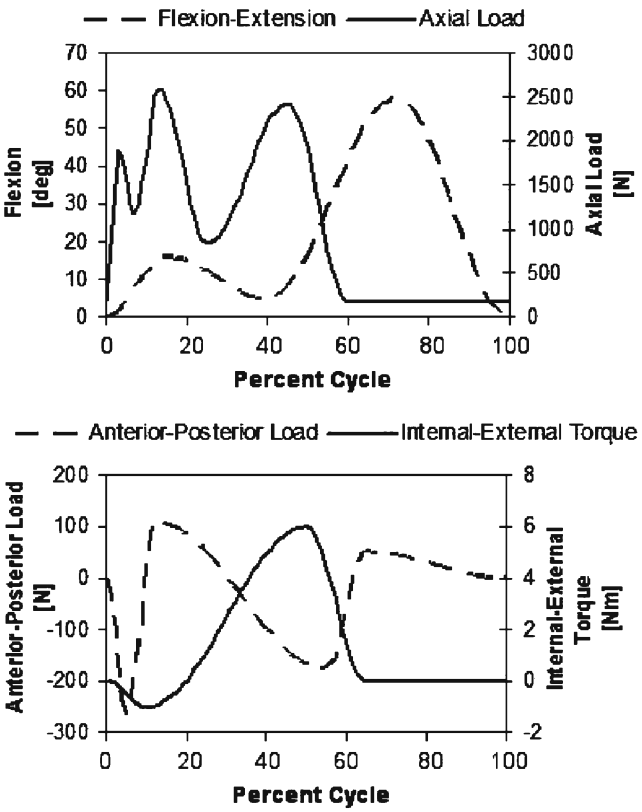

Fig. 6 Load and displacement waveforms used for wear testing with ISO-14243-1, which is simulated in this study

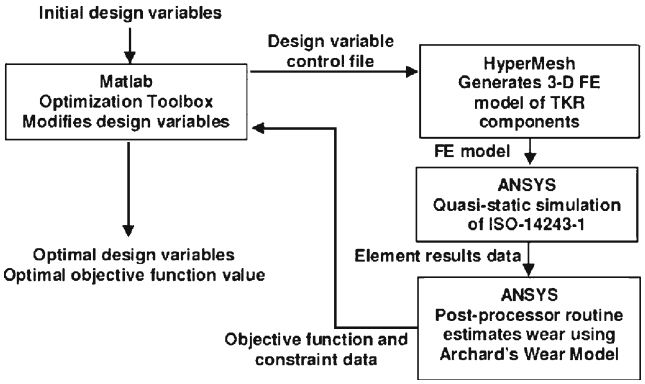

Fig. 7 Process flow for TKR design optimization using Matlab, HyperMesh and ANSYS

as well as anterior-posterior load are prescribed at the pilot node of the femoral component. All other degrees of freedom at this node are constrained. Internal-external torque and axial load are applied to the pilot node of the UHMWPE insert. Anterior-posterior displacement is constrained at this node, but all remaining degrees of freedom are left unconstrained. The load and displacement profiles outlined in the ISO standard are discretized into 80 intervals for use in quasi-static FEM simulations.

2.4 Wear model

There is currently no analytical model that can accurately predict wear. However, a modified version of Archard's wear model (Archard and Hirst 1956; Marshek and Chen 1989) – which states that wear is a function of contact pressure, contact area, sliding distance, and a wear coefficient k – is known to be able to predict wear with reasonable accuracy if a proper value of k is found experimentally (Hamilton 2001; Maxian et al. 1996a). Further details are discussed in Section 4. The modified Archard's wear model states:

$$W_{vol} = \iint k\sigma \, ds \, dA \tag{1}$$

where W_{vol} is the volumetric wear, k is the wear coefficient, σ is the contact pressure, s is the sliding distance and A is the contact area.

For use with FE contact analysis with multiple load steps, in this study the following equation is used:

$$W_{vol} = \sum_{loadsteps} \left[\sum_{elements} (k \times \sigma_{elem} \times s_{elem} \times A_{elem}) \right] \tag{2}$$

where W_{vol} is the volumetric wear, k is the wear coefficient, σ_{elem} is the contact pressure, s_{elem} is the sliding

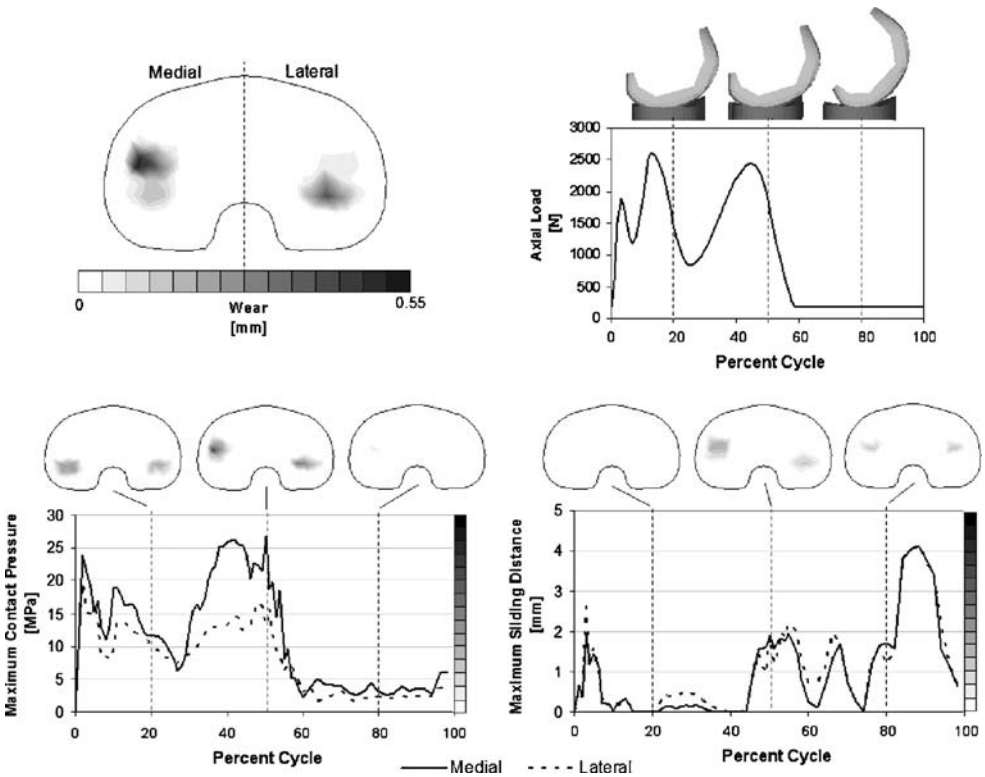

Fig. 8 Medial/lateral wear for initial design, as well as contact pressure and sliding distance at selected instances of FE simulation. Axial load is shown for reference

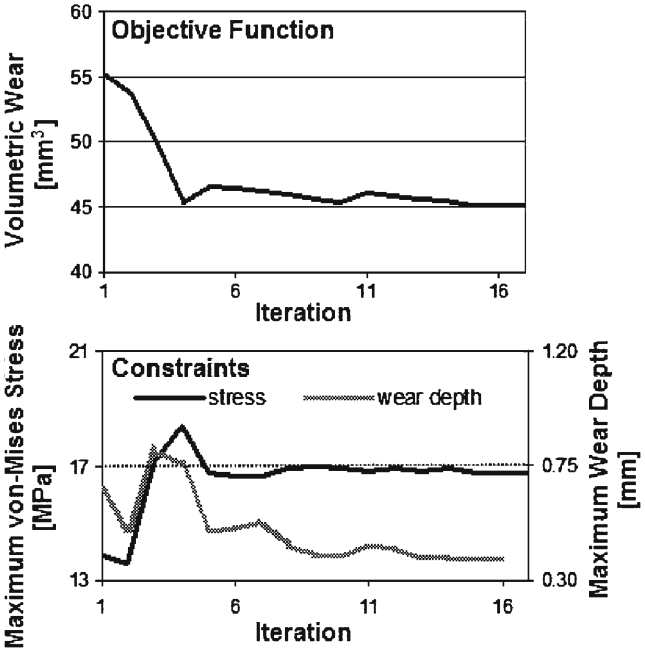

Fig. 9 Objective function (wear) and constraint (maximum von-Mises stress, maximum wear depth) history

distance and A_{elem} is the area of a contact element during a loadstep.

The wear coefficient k used in this study is 10.656×10^{-7} mm^3/Nm, which has been used in previous literature for simulating total joint arthroplasties (Hamilton 2001; Maxian et al. 1996a).

2.5 Design optimization

We select UHMWPE wear as the objective function; a mathematical problem statement is then developed which outlines the equality and inequality constraints, as well as the design variables.

The wear is most greatly affected by the variables which describe the contacting surfaces. These 10 design parameters are selected for optimization—the radii of the femoral condyles in the frontal plane (RF-med, RF-lat), the distal and posterior radii of the femoral condyles in the sagittal plane (RD-med, RD-lat, RP-med, RP-lat), the distance from the implant mid-line along a medial-lateral axis to the lowest point of the femoral condyles (W-med, W-lat) and the conformity between the femoral condyles and dished out surfaces of the UHMWPE insert in the frontal (C-fr) and sagittal (C-sa) planes. This controls the difference between the corresponding radii of curvature in a particular plane (radius of insert geometry minus radius of femoral component geometry), where conforming means the radii of curvature are nearly identical (within 5 mm frontal, 15 mm sagittal) and non-conforming means the radii of curvature differ greatly (up to 45 mm frontal, 55 mm sagittal). Conformity has been normalized to between 0 and 1, where 0 is minimal conformity and 1 is maximum conformity, in a particular plane. Design variable limits are selected which allow model and mesh quality to be maintained for any particular design (to avoid distorted meshes and possibly innaccurate results). The initial design geometry is based on Zimmer NexGen CR implant components.

Optimization is performed in order to yield the best design with respect to the objective function (volumetric wear), subject to the maximum von-Mises stress in the UHMWPE insert remaining below 17 MPa and the maximum wear depth remaining below 0.75 mm per year, where a year is assumed to be 10^6 cycles. The non-linear compressive material model derived from work by Cripton (1993) exhibits decreasing stiffnesses until stresses of 17 MPa. This value was selected as the maximum allowable von-Mises stress, slightly lower than the 5% yield stress for UHMWPE. To prevent designs where unreasonably large wear depths exist, even with low volumetric wear, a maximum wear depth of 0.75 mm per 10^6 cycles is selected. We describe the design problem mathematically as:

$$\begin{aligned} &\textbf{Minimize } W_{vol}(\boldsymbol{x}) \\ &\text{subject to } \sigma_{von\text{-}mises\text{-}max}(\boldsymbol{x}) \leq 17 \text{ MPa} \\ &\qquad \delta_{max}(\boldsymbol{x}) \leq 0.75 \text{ mm} \\ &\qquad (x_i)_{min} \leq x_i \leq (x_i)_{max} \end{aligned} \tag{3}$$

where W_{vol} [mm^3] is the predicted volumetric wear after 10^6 cycles, x_i are normalized values controlling the design variables RF-med [mm], RF-lat [mm], RD-med [mm], RD-lat [mm], RP-med [mm], RP-lat [mm],

Table 1 Initial versus optimum design

	Design variables										Results		
	RF-med [mm]	RF-lat [mm]	RD-med [mm]	RD-lat [mm]	RP-med [mm]	RP-lat [mm]	W-med [mm]	W-lat [mm]	C-fr -	C-sa -	Wear [mm^3]	Depth [mm]	Stress [MPa]
Initial	47.50	47.50	52.50	52.50	27.50	27.50	23.50	23.50	0.5	0.5	55.248	0.653	13.88
Optimum	56.01	57.85	68.24$^+$	37.30$^-$	16.88	16.43$^-$	20.60$^-$	21.98	0.06$^-$	0.20	45.013	0.387	16.77

W-med [mm], W-lat [mm], C-fr, and C-sa. $\sigma_{von\text{-}mises\text{-}max}$ [MPa] is the maximum von-Mises stress in the insert and δ_{max} [mm] is the maximum wear depth at the contact surface.

In our study, we use the Optimization Toolbox for Matlab v 7 (The MathWorks Inc., Natick, MA.) as our optimizer for performing gradient based optimization using the steepest descent method. Design parameters are sent to the pre-processor, HyperMesh, which generates the FE model for wear testing simulation in ANSYS. The post-processing routine which runs within ANSYS calculates the volumetric wear predicted by Archard's wear model, as well as the maximum damage depth and von-Mises stress. This information is passed back to Matlab where the optimization routine begins another iteration (Fig. 7).

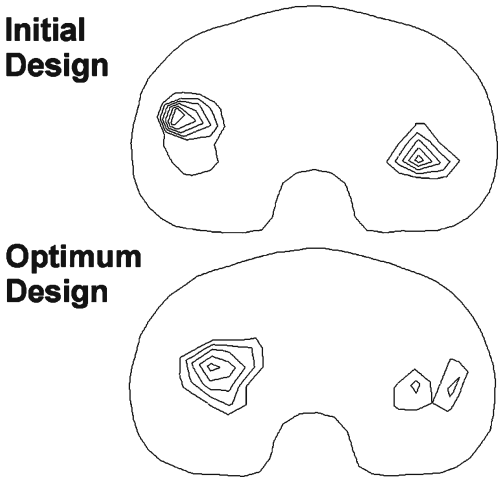

Fig. 11 Wear distribution across surface of UHMWPE insert. Iso-lines placed at 0.075 mm increments. It should be noted these plots show averaged data, so the maximum wear depth is slightly lower than reported in Table 1

3 Results

3.1 FEA results

A FEA of the initial design simulates the wear test and predicts the wear resulting from 10^6 cycles. Figure 8 shows the maximum medial and lateral contact pressures and sliding distances during specific instances of the gait cycle, the two components contributing to wear when using Archard's wear model. The predicted wear for this design is 55.248 mm^3 and a maximum wear depth of 0.653 mm, per 10^6 cycles. The maximum von-Mises stress within the UHMWPE insert is 13.88 MPa. The wear distribution depicted in Fig. 8 shows node-averaged data, so magnitudes do not agree with the maximum integration point wear depth criterion for the wear depth constraint.

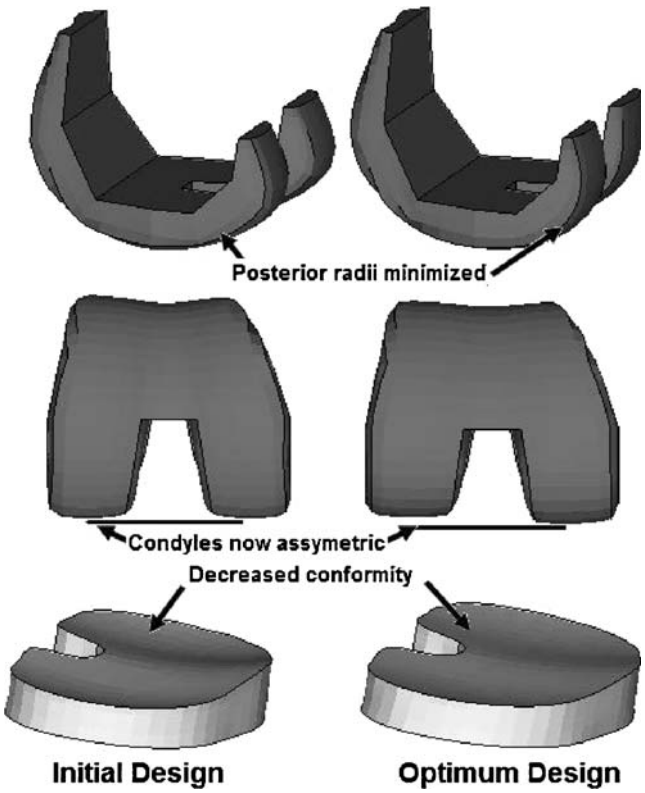

Fig. 10 Comparison of initial and optimum shapes. Posterior radii and conformity are reduced, and femoral condyles become assymetric as the medial distal radius is maximized and lateral distal radius is minimized

3.2 Optimization results

Shape optimization is performed and a design optimized for minimal wear is generated. Figure 9 shows the objective function and constraint histories during the optimization process. The optimum design is converged upon at design iteration number 17. The stress criterion is satisfied but very close to the limit, while maximum wear depth is well below the constraint. Comparing to the initial design, the optimized design reduces the expected wear by 18.5%, to a wear of 45.013 mm^3 per 10^6 cycles. The maximum wear depth decreases from 0.653 to 0.387 mm, −40.7%, while maximum von-Mises stress approaches the allowable limit.

The difference between initial and optimum design variable values can be seen in Table 1, and are depicted in Fig. 10 . Most design variables meet their most extreme values, which is denoted in the table with superscript as (+) for a maximum and (−) for a minimum.

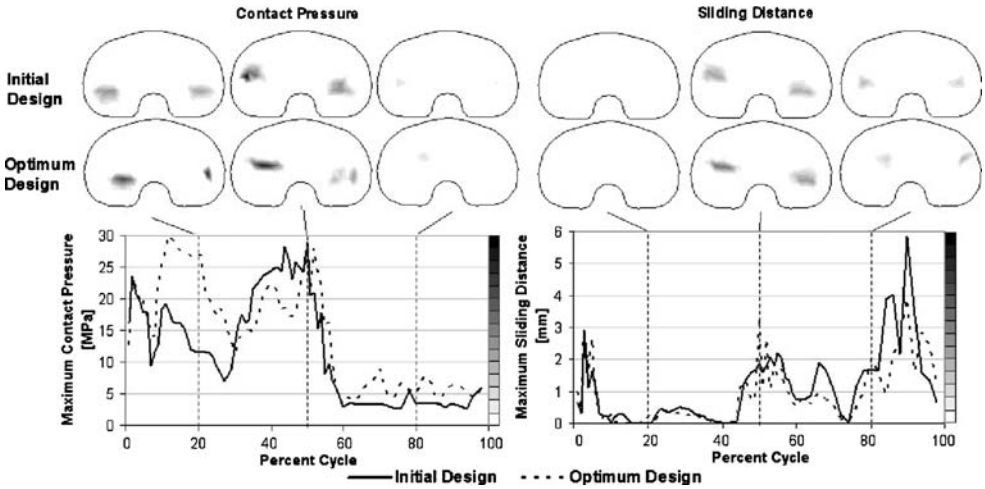

Fig. 12 Comparison of contact pressure and sliding distance contours and maximum values during gait cycle for initial and optimum design

Changing the shape of the two contacting surfaces changes the wear distribution over the surface of the UHMWPE insert as well as the total amount of wear. Figure 11 depicts the wear depth contours across the surfaces, and Fig. 12 shows how the contributors to wear – contact pressure and sliding distance – differ for the initial and optimum design. It should be noted that the maximum wear depths do not match the values of Table 1, where absolute maximum integration point values were used versus the node averaged data shown in Fig. 11. The wear patches in the optimum design are less severe, and are significantly smaller in size. Due to the smaller wear patches, the total volumetric wear at the interface is lower.

4 Discussion

The polyethylene properties used in this study did not include the effects of creep. It is recognized that creep and plasticity effects may cause surface deformation, most significantly early on in the implant's *in-vivo* lifespan or where high contact stresses are present. For the purpose of this analysis, however, creep is assumed to be minimal and the effects are neglected.

The modified version of Archard's classic wear law (Archard and Hirst 1956; Marshek and Chen 1989) used in this study was originally derived for the prediction of wear from contacting metal surfaces, but good agreement with *in-vitro* polyethylene wear testing has been reported (Maxian et al. 1996a, b, c, 1997) showing that Archard's wear law is a better tool for predicting wear compared to only contact pressure evaluation.

The wear coefficient k is an experimentally determined factor, most dependent on the material pairing and surface roughness (Fisher et al. 1994). Values from 2.20×10^{-7} mm^3/Nm (Fregly et al. 2005) to 10.656×10^{-7} mm^3/Nm (Hamilton 2001; Maxian et al. 1996a) have been reported for TJA. While wear values found in this research appear relatively high, since the wear factor is simply a scalar multiplier on the wear volume, the optimization trend did not depend on the accuracy of this value, which will later be experimentally determined for this pairing.

In general, the wear optimized design decreases the radii of curvature of the femoral condyles in the sagittal plane and increases radii in the frontal plane, as well as reducing the amount of conformity between the femoral condyles and the polyethylene insert. These changes in geometry are expected to alter the nature of the articulation, causing medial-lateral line contact. The smaller product of contact area and sliding distance would offset the effects of the increased contact pressures, reducing volumetric wear. Essner et al. (2003) observed this trend in a study on TKR component conformity; although more studies would be needed to have statistical significance. This behaviour, however, may be violated for exceedingly high contact pressures which could introduce alternative failure modes not addressed by the present wear model.

For the first time, the shape of a TKR was optimized in three-dimensions for wear reduction, while considering the entire gait cycle using ISO wear testing standards. The expected polyethylene wear was reduced by 18.5% by reducing the radii of curvature of the femoral condyles in the sagittal plane, increasing the radii of curvature in the frontal plane, and reducing the conformity between the femoral component and the UHMWPE insert. This design provides medial-lateral line contact patches, and a smaller contact area

between the two components which decreases the volume of abrasive wear debris. The reduction in the wear of the polyethylene would contribute to longer implant life and reduced chance of loosening.

There are several limitations to the current study, including assumptions in the wear model, no account for variability, the elimination of any kinematic assessment and sizing issues. The future work includes the study on the impact of the geometry changes on range of motion and stability of the joint, while in this work the loading prescribes a range of motion rather than determining the resulting displacement from muscle loads. If range of motion or stability were to be optimized, a completely separate modeling and analysis has to be performed using a rigid body dynamics module, with springs to represent ligaments and soft tissue constraints and muscle forces applied rather than prescribed motions. Different loading conditions and knee sizes should also be considered in order to reflect the variability implants see *in-vivo*. This design is optimized for the loading conditions of the standardized wear test, however patient specific implants could also be designed, optimized for the specific loading, size and activity level of the candidate. Despite these limitations, it has been shown that design optimization is an effective tool for TKR design, and future analyses will consider wider evaluation criteria in order to perform multidisciplinary and multiobjective optimization.

Acknowledgements The authors would like to thank Dr. Derek Cooke of OAISYS Inc. and Dr. Danny Levine of Zimmer Inc. for their valuable feedback.

References

ANSYS (2004) ANSYS Theory Reference 9.0. ANSYS, Canonsburg

Archard JF, Hirst W (1956) The wear of metals under unlubricated conditions. Proc R Soc Lond Ser A 236:397–410

Au AG, Liggins AB, Raso VJ, Amirfazli A (2005) A parametric analysis of fixation post shape in tibial knee prostheses. Med Eng Phys 27:123–134

Bills P, Brown L, Jiang X, Blunt L (2005) A metrology solution for the orthopaedic industry. J Phys Conf Ser 13:316–319

Cornwall GB, Bryant JT, Hansson CM, Rudan J, Kennedy LA, Cooke TDV (1995) A quantitative technique for reporting surface degradation patterns of UHMWPE components of retrieved total knee replacements. J Appl Biomater 6:9–18

Cripton PA (1993) Compressive characterization of ultra high molecular weight polyethylene with applications to contact stress analysis of total knee replacements. M.Sc. Thesis, Department of Mechanical and Materials Engineering, Queen's University

Dargahi J, Najarian S, Amiri S (2003) Optimization of the geometry of total knee implant in the sagittal plane using FEA. Bio-Med Mater Eng 13:439–449

Essner A, Klein R, Bushelow M, Wang A, Kvitnitsky M, Mahoney O (2003) The effect of sagittal conformity on knee wear. Wear 255:1085–1092

Fisher J, Dowson D, Hamdzah H, Lee HL (1994) Effect of sliding velocity on the friction and wear of UHMWPE for use in total artificial joints. Wear 175:219–225

Fregly BJ, Sawyer WG, Harman MK, Banks SA (2003) Experimental evaluation of an elastic foundation model to predict contact pressures in knee replacements. J Biomech 36: 1659–1668

Fregly BJ, Sawyer WG, Harman MK, Banks SA (2005) Computational wear prediction of a total knee replacement from in vivo kinematics. J Biomech 38:305–314

Giddings VL, Kurtz SM, Edidin AA (2001) Total knee replacement polyethylene stresses during loading in a knee simulator. J Tribol 123:842–847

Godest AC, Beaugonin M, Haug E, Taylor M, Gregson PJ (2002) Simulation of a knee joint replacement during a gait cycle using explicit finite element analysis. J Biomech 35: 267–275

Halloran JP, Petrella AJ, Rullkoetter PJ (2005) Explicit finite element modeling of total knee replacement mechanics. J Biomech 38:323–331

Hamilton MA (2001) Development of a computational tool to predict wear in UHMWPE tibial bearings: STLE scholarship award winner. Department of Mechanical and Materials Engineering, University of Florida

International Organization for Standardization (1999) ISO/Draft International Standard 14243-1. Wear of total knee prostheses, Part 1: Loading and displacement for wear testing machines and corresponding environmental conditions for test. International Organization for Standardization, Genéve

Johnson KL (1985) Contact mechanics. Cambridge University Press, Cambridge, pp. 90–93

Knight LA, Pal S, Coleman JC, Bronson F, Haider H, Levine DL, Taylor M, RUllkoetter PJ (2007) Comparison of long-term numerical and experimental total knee replacement wear during simulated gait loading. J Biomech 40: 1550–1558

Kurtz S, Lau E, Zhao K, Mowat F, Ong K, Halpern M (2006) The future burden of hip and knee revisions: U.S. projections from 2005 to 2030. Annu Meet AAOS 73:SE53

Marshek KM, Chen HH (1989) Discretization pressure-wear theory for bodies in sliding contact. J Tribol 111:95–100

Maxian TA, Brown TD, Pedersen DR, Callaghan JJ (1996a) 3-Dimensional sliding/contact computational simulation of total hip wear. Clin Orthop Relat Res 333:41–50

Maxian TA, Brown TD, Pedersen DR, Callaghan JJ (1996b) Adaptive finite element modeling of long-term polyethylene wear in total hip arthroplasty. J Orthop Res 14: 668–675

Maxian TA, Brown TD, Pedersen DR, Callaghan JJ (1996c) A sliding-distance-coupled finite element formulation for polyethylene wear in total hip arthroplasty. J Biomech 29: 687–692

Maxian TA, Brown TD, Pedersen DR, McKellop HA, Lu B, Callaghan JJ (1997) Finite element analysis of acetabular wear. Clin Orthop Relat Res 344:111–117

McEwen HMJ, Barnett PI, Bell CJ, Farrar R, Auger DD, Stone MH, Fisher J (2005) The influence of design, materials and kinematics on the in vitro wear of total knee replacements. J Biomech 38:357–365

Revell PA, Weightman B, Freeman MAR, Roberts BVER (1978) The production and biology of polyethylene wear debris. Arch Orthop Trauma Surg 91:167–181

Sathasivam S, Walker PS (1994) Optimization of the bearing surface geometry of total knees. J Biomech 27:255–264

Sathasivam S, Walker PS (1998) Computer model to predict subsurface damage in tibial inserts of total knees. J Orthop Res 16:564–571

Sharkey PF, Hozack WJ, Rothman RH, Shastri S, Jacoby SM (2002) Insall award paper: why are total knee arthroplasties failing today? Clin Orthop Relat Res 404:7–13

Zimmer.com (2007) Zimmer Incorporated. http://www.zimmer.com. Accessed 23 July 2007

Zhao D, Sakoda H, Sawyer WG, Banks SA, Fregly BJ (2008) Predicting knee replacement damage in a simulator machine using a computational model with a consistent wear factor. J Biomech Eng. doi:10.1115/1.2838030